Selective quantum evolution of a qubit state due to continuous measurement

Korotkov

Sept. 18, 2000

Abstract

We consider a two-level quantum system (qubit) which is continuously measured by a detector. The information provided by the detector is taken into account to describe the evolution during a particular realization of the measurement process. We discuss the Bayesian formalism for such "selective" evolution of an individual qubit and apply it to several solid-state setups. In particular, we show how to suppress qubit decoherence using continuous measurement and a feed- back loop.

1. Introduction

Studies of two-level quantum systems have acquired recently a new meaning related to the use of this simple quantum object as an elementary cell (qubit) of a quantum computer. [1] This paper addresses the measurement of a qubit state, so it necessarily touches the long-standing and still somewhat controversial problem of quantum measurement, [2-4] which is known under the name of quantum state "collapse".

Having in mind a solid-state realization of qubit (for different proposals see, e.g., Refs.[5-9]) let us emphasize that a realistic detector has a noisy output signal, so the measurement of a qubit state should necessarily have finite duration in order to provide an acceptable signal- to-noise ratio. In this situation the "orthodox" collapse postulate [10-12] cannot be applied directly, since the measurement is not instantaneous. The necessity of a more general formalism is obvious, for example, in the case when the qubit "self-evolution" changes the quantum state considerably during a measurement process. Even if there is no self-evolution, one can wonder what happens with the qubit state after a partially completed measurement (when the signal-to-noise ratio is still on the order of unity). So, we need a formalism to describe the gradual qubit evolution, caused by the measurement process. As will be discussed later, the Schrödinger equation alone is not sufficient for the complete description of this evolution, and should be complemented by a slightly generalized collapse principle.

Continuous quantum measurement was a subject of ex- tensive theoretical analysis during last two decades, and there are two main approaches to this

problem. One approach is based on the theory of interaction with a dissipative environment. [13,14] Taking the trace over the numerous degrees of freedom of the detector, it is possible to obtain a gradual evolution of the measured system density matrix from the pure initial state to the incoherent statistical mixture, thus describing the measurement process. [15,16] Since the procedure implies an averaging over the *ensemble*, the final equations of this formalism are deterministic and can be derived from the Schrödinger equation alone, without any notion of state collapse. The success of the theory in describing many solid-state experiments has supported an opinion common nowadays that the collapse principle is a needless part of quantum mechanics. Because of the dominance of this approach (at least in the solid-state community) we will call it "conventional".

The other general approach to continuous quantum measurement (see, e.g., Refs.[17-36]) explicitly or implicitly uses the idea of the state collapse. Since quantum measurement is a fundamentally indeterministic process so that the exact measurement result is typically unpredictable, the approach describes the random evolution of the quantum state of the measured system. The important advantage in comparison with the conventional approach is the absence of averaging over the total ensemble; hence, it is possible to describe the evolution of an *individual* quantum system during a particular realization of the measurement process. The evolution of the measured system obviously depends on a particular measurement outcome; in other words, it is selected by (conditioned on) the measurement result. So, this approach is usually called the approach of *selective* or *conditional* quantum evolution. There is a rather broad variety of formalisms and their interpretations within the approach. [17-36] Depending on the details of the studied measurement setup and applied formalism, different authors discuss quantum trajectories, quantum state diffusion, stochastic evolution of the wavefunction, quantum jumps, stochastic Schrödinger equation, complex Hamiltonian, method of restricted path integral, Bayesian formalism, etc. (for comparison between several different ideas see, e.g., Ref. [19]). The approach of selective quantum evolution is relatively well developed in quantum optics; in contrast, it was introduced into the context of solid-state mesoscopics only recently. [33]

In the present paper we continue the development of the Bayesian formalism [33,35-38] for selective quantum evolution of a qubit due to continuous measurement. Several issues of the formalism derivation and interpretation are

explained in more detail than in previous papers. A new way of derivation is presented for a special case of low- transparency quantum point contact (tunnel junction) as a detector. We also discuss equations (briefly mentioned in Ref. [35]) for the evolution of a qubit measured by single-electron transistor, which go beyond the approximation used for a nonideal detector in Ref.33. Special attention is paid to a regime outside the "weakly responding" limit. Finally, we discuss the operation of a quantum feedback loop which can suppress the qubit decoherence caused by interaction with the environment.

2. Examples of Measurement Setup

The total Hamiltonian $\mathcal{H}$ of a qubit continuously measured by a detector,

$$\mathcal{H} = \mathcal{H}_{QB} + \mathcal{H}_{DET} + \mathcal{H}_{INT} \tag{1}$$

consists of terms describing the qubit, the detector, and their interaction. The qubit hamiltonian,

$$\mathcal{H}_{QB} = \frac{\varepsilon}{2}(c_1^\dagger c_1 - c_2^\dagger c_2) + H(c_1^\dagger c_1 - c_2^\dagger c_2) \tag{2}$$

is characterized by the energy asymmetry ε between two levels and the mixing (tunneling) strength H (we assume real H without loss of generality). The Hamiltonian (2) is written in the basis defined by the coupling with the detector. We will refer to mutually orthogonal states $|1\rangle$ and $|2\rangle$ as "localized" states in order to distinguish them from the "diagonal" basis consisting of the ground and excited states, which differ in energy by $\hbar\Omega = (4H^2 + \varepsilon^2)^{1/2}$.

2.1. Double-dot measured by tunnel junction

Our study will be applicable to several different types of qubits and detectors. As the main example we con- sider a double quantum dot occupied by a single electron, the position of which is measured by a low-transparency tunnel junction nearby (see Fig. 1).
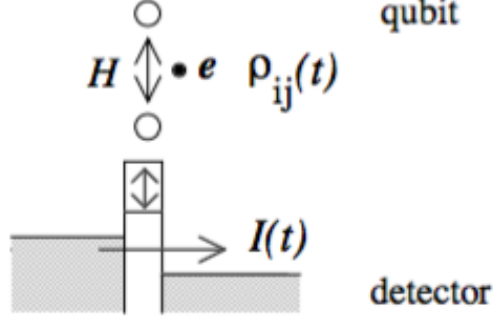
Figure 1: Tunnel junction as a detector of the electron position in the double-dot which affects the barrier height. The current $I(t)$ (detector output) reflects the evolution of the density matrix $\rho_{ij}(t)$ of the measured two-level system (qubit).

Basically following the model of Ref. [39] let us assume that the tunnel barrier height depends on the location of the electron in either dot 1 or 2; then the current through the tunnel junction (which is the detector output) is sensitive to the electron location. In this case the detector and interaction Hamiltonians can be written as

$$\mathcal{H}_{DET} = \sum_l E_l a_l^\dagger a_l + \sum_r E_r a_r^\dagger a_r + \sum_{l,r} T(a_r^\dagger a_l + a_l^\dagger a_r)$$

$$\mathcal{H}_{INT} = \sum_{l,r} \frac{\Delta t}{2} \sum_l E_l a_l^\dagger a_l (a_r^\dagger a_l + a_l^\dagger a_r) \tag{3}$$

where both T and ΔT are real and their dependence on the states in electrodes (l, r) is neglected. If the electron occupies dot 1, then the average current through the detector is $I_1 = 2\pi(T + \Delta T/2)^2 \rho_l \rho_r e^2 V / \hbar$ (V is the voltage across the tunnel junction and $\rho_{l,r}$ are the densities of states in the electrodes) while if the measured electron is in the dot 2, the average current is $I_2 = 2\pi(T - \Delta T/2)^2 \rho_l \rho_r e^2 V / \hbar$.

The difference between the currents,

$$\Delta I \equiv I_1 - I_2 \tag{4}$$

determines the detector response to the electron position (notice the different sign in the definition of ΔI used in Ref. [33]). Because of the finite noise of the detector current $I(t)$, the two states of the system cannot be distinguished

4

instantaneously and the signal-to-noise ratio gradually improves with the increase of the measurement duration. Let us define the typical measurement time τ_m necessary to distinguish between two states as the time for which the signal-to-noise ratio is close to unity: [40]

$$\tau_m = \frac{(\sqrt{S_1} + \sqrt{S_2})^2}{2(\Delta I)^2} \tag{5}$$

where S_1 and S_2 are the low-frequency spectral densities of the detector noise for states $|1\rangle$ and $|2\rangle$. (As will be seen later, τ_m also determines the timescale for selective evolution of the qubit state due to measurement.) For a low-transparency tunnel junction $S_{1,2} = 2eI_{1,2} \coth(\beta eV/2)$, where β is the inverse temperature. At sufficiently small temperatures $\beta^{-1} \ll eV$ (we assume zero temperature unless specially mentioned) the detector shot noise is given by the Schottky formula,

$$S_{1,2} = 2eI_{1,2} \tag{6}$$

To avoid an explicit account of the detector quantum noise we will consider only processes at frequencies $\omega \ll eV/\hbar$ (in particular, we assume $\tau_m^{-1} \ll eV/\hbar$).

The major part of the paper will be devoted to the detector in the "weakly responding" regime when two states of the detector differ only a little (one can also call this regime "linear", while the term "weak coupling" is reserved for a different meaning), in particular,

$$|\Delta I| \ll I_0 \quad , \quad I_0 \equiv \frac{I_1 + I_2}{2} \tag{7}$$

$$|S_1 - S_2| \ll S_0 \quad , \quad S_0 \equiv \frac{S_1 + S_2}{2} \tag{8}$$

so the typical measurement time is

$$\tau_m = \frac{2S_0}{(\Delta I)^2} \tag{9}$$

For a weakly responding detector the timescale e/I_0 of individual electron passages through the detector is much shorter than τ_m, so the current can be considered continuous on the measurement timescale.

2.2. Double-dot and quantum point contact

Besides the low-transparency tunnel junction as a de- tector, we can also consider a quantum point contact with arbitrary transparency $\mathcal{T}$ which depends on the electron position in the double dot. This setup in the context of continuous quantum measurement has been extensively studied both experimentally [41,42] and theoretically. [43-48] In spite of a somewhat different mathematical description (we will not write the Hamiltonian explicitly) this case is very close to the case above, which we prefer because of its simplicity. The obvious new feature is the different formula for the shot noise, [49]

$$S_{1,2} = 2eI_{1,2}(1 - \mathcal{T}_{1,2}) \tag{10}$$

where $I_{1,2} = -\mathcal{T}_{1,2}e^3V/\pi\hbar$. Notice that for the quantum point contact as a detector we make the condition (7) for weakly responding regime a little stronger, $|\Delta I| \ll (1-\mathcal{T}_{1,2})I_{1,2}$, so that both transmitted and reflected currents can be considered continuous on the measurement timescale.

2.3. Cooper-pair box and single-electron transistor

Another interesting measurement setup (Fig. 2) introduced in Ref. [50] in the context of a solid-state quantum computer, is a single-Cooper-pair box measured by a single-electron transistor (a somewhat similar setup has been recently used for the experimental demonstration [51] of quantum oscillations in the time domain).
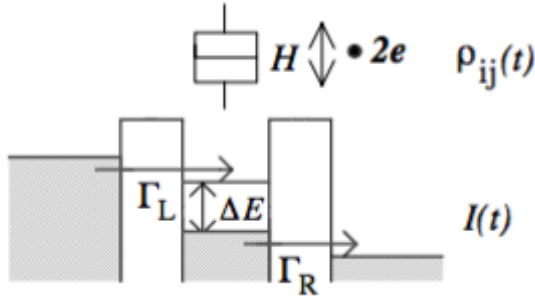

Figure 2: Single-electron transistor (detector) measuring the charge state of the single-Cooper-pair box (qubit).

The qubit in this case is represented by two charge states of a small- capacitance Josephson junction. The Josephson coupling provides the matrix

element H in Eq. (2) which is assumed to be much smaller than the single-electron charging energy, so that only two charge states (adjusted by the gate voltage to be close in energy) are important. The capacitively coupled single-electron transistor is sensitive to the charge state of the Cooper-pair box and serves as the detector; the current $I(t)$ through the transistor is the measurement output.

One can find the detailed discussion of the Hamiltonian for this measurement setup in Ref. [50]. The qubit state affects the energy of the middle island of the single-electron transistor (Fig. 2), so the interaction is of "density-density" type:

$$H_{INT} = \frac{\Delta E}{2}(c_2^\dagger c_2 - c_1^\dagger c_1)\left(\sum_m a_m^\dagger a_m - \text{ constant}\right) \tag{11}$$

where the factor in large brackets is the number of extra electrons on the transistor island. In the "orthodox" regime of sequential single-electron tunneling [52,53] in the transistor, the energy change ΔE affects the rates of tunneling through the two tunnel junctions and thus affects the average current I. In the simplest case when the electrons can tunnel only in a strict alternating sequence with rates Γ_L and Γ_R, the average currents I_1 and I_2 can be calculated as [52]

$$I_i = \frac{e\Gamma_{L,i}\Gamma_{R,i}}{\Gamma_{L,i} + \Gamma_{R,i}} \tag{12}$$

where $i = 1, 2$ corresponds to the charge state of the qubit. Well outside the Coulomb blockade range the difference between the rates is $\Gamma_{R,2} - \Gamma_{R,1} = \Delta E/e^2 R_R$, where $R_{L(R)} \gg \hbar/e^2$ are the resistances of tunnel junctions.

The measurement time to distinguish between states $|1\rangle$ and $|2\rangle$ for this setup is given by Eq. (5), in which the spectral density of the single-electron transistor cur- rent can be calculated using equations of Refs. [54,55] (the Schottky formula used for this purpose in Ref. [50] is valid only in a limiting case). In the special case corresponding to Eq. (12) the shot noise is given by the formula [55]

$$S_i = \frac{2eI_i(\Gamma_{L,i}^2 + \Gamma_{R,i}^2)}{(\Gamma_{L,i} + \Gamma_{R,i})^2} \tag{13}$$

2.4. Two SQUIDS

One more solid-state realization of continuous quantum measurement of a qubit can be done using two flux states of a SQUID as a qubit and another inductively coupled SQUID as a detector. [56] The corresponding Hamiltonian and calculations of the SQUID noise can be found, e.g., in Ref. [57]. A minor difference in the formalism is related to the fact that the typical output signal from a SQUID is voltage instead of current in the examples above.

3. Results of the Conventional Approach

The goal of the present paper is the analysis of a selective evolution of the qubit state due to continuous measurement, taking into account the detector output $I(t)$. However, before that let us review the results of the conventional approach [39,43-48,50] to this problem which does not take into account the detector output.

We describe the quantum state of a qubit by the density matrix ρ_{ij} in the basis of localized states $|1\rangle$ and $|2\rangle$, so that ρ_{ii} ($\rho_{11} + \rho_{22} = 1$) is the probability to find the system in the state "i" if an instantaneous measurement in this basis is performed, while ρ_{12} ($\rho_{21} = \rho_{12}^*$) characterizes the coherence; in particular, $|\rho_{12}|^2 = \rho_{11}\rho_{22}$ corresponds to a pure state. In the conventional approach [13] the evolution of ρ_{ij} is calculated using the Schrödinger equation for the combined system including the detector and then tracing out the detector degrees of freedom that leads to the following equations:[39,43-48,50]

$$\dot{\rho}_{11} = -\dot{\rho}_{22} = -2\frac{H}{\hbar}\operatorname{Im}\rho_{12} \qquad (14)$$

$$\dot{\rho}_{12} = i\frac{\varepsilon}{\hbar}\rho_{12} + i\frac{H}{\hbar}(\rho_{11} - \rho_{22}) - \Gamma_d\rho_{12} \qquad (15)$$

where the effect of continuous measurement is described by the ensemble decoherence rate Γ_d. (Such equations in similar problems when the environment causes dephasing are known for many years — see, e.g., Refs. [13,58,59]).

For a double-dot measured by a tunnel junction (Fig. 1) the decoherence

rate has been obtained in Ref. [39]:

$$\Gamma_d = \frac{(\sqrt{I_1} - \sqrt{I_2})^2}{2e} \qquad (16)$$

Comparing this equation with Eqs. (5) and (6) one can easily notice that Γ_d has a direct relation to the typical measurement time τ_m:

$$\Gamma_d = (2\tau_m)^{-1} \qquad (17)$$

This relation obviously remains valid in the weakly re- sponding regime when the decoherence rate can be expressed as

$$\Gamma_d = \frac{(\Delta I)^2}{4S_0} \qquad (18)$$

In the case of a finite-transparency quantum point contact as a detector [41-48] the ensemble decoherence rate has been mainly studied in the weakly responding regime. The most important for us result [41-43,46-48] is that for symmetric coupling Eq. (18) is still valid, just the shot noise is now given by Eq. (10) instead of Eq. (6) (as mentioned, the temperature is zero). In the asymmetric case, if the phase of transmitted and reflected electrons in the detector is sensitive to states $|1\rangle$ and $|2\rangle$, then there is an extra term in the equation for the decoherence rate, so the decoherence is faster [42,45,47,48] than given by Eq. (18).

The inequality $\Gamma_d > (2\tau_m)^{-1}$ has been also obtained in Ref.50 for a single-electron transistor measuring a single-Cooper-pair box. The interaction Hamiltonian (11) allows us to relate the dephasing rate, $\Gamma_d = (\Delta E)^2 S_m / 4\hbar^2$, to the low-frequency spectral density S_m of the fluctuating number m of extra electrons on the transistor central island. These fluctuations have been calculated in Refs. [54,55] within the framework of the orthodox theory. [52] In particular, assuming the weakly responding regime and the two-charge-state dynamics corresponding to Eqs. (12)-(13) we obtain [37,60]

$$\Gamma_d = \frac{(\Delta E)^2 \Gamma_L \Gamma_R}{\hbar^2 (\Gamma_L + \Gamma_R)^3} \qquad (19)$$

(notice a different expression in Ref. [50]). In this case

$$2\Gamma_d \tau_m = \frac{8\Gamma_L^2 \Gamma_R^2 (\Gamma_L^2 + \Gamma_R^2)}{(\Gamma_L + \Gamma_R)^2 (\Gamma_L^2 \hbar / eR_R - \Gamma_R^2 \hbar / eR_L)} \qquad (20)$$

9

so for

$$2\Gamma_d \tau_m = 8 \left(\frac{\Gamma_L}{\Gamma_R}\right)^2 \left(\frac{R_L e^2}{\hbar}\right)^2 \tag{21}$$

Formally this expression becomes less than one if $e^2\Gamma_L R_L < \hbar\Gamma_R/\sqrt{8}$; however, in this case the significant cotunneling makes the orthodox approach invalid and the quantum noise contribution becomes important. [54] In the cotunneling regime (well below the Coulomb blockade threshold) Γ_d should be obviously comparable to $(2\tau_m)^{-1}$ because in this case essentially the barrier height (the energy of the virtual state) is sensitive to a measured state, so the detecting principle becomes similar to the case of Fig. 1. The inequality $\Gamma_d \geq (2\tau_m)^{-1}$ should remain valid in the cotunneling regime as well; this fact will be obvious from the Bayesian formalism.

The quantum backaction of a SQUID in the linear-response approximation was calculated in Ref. [61]. It was shown that the total energy sensitivity of a SQUID $(\epsilon_I \epsilon_V - \epsilon_{IV}^2)^{1/2}$ (which takes the backaction into account) is limited by $\hbar/2$. Here ϵ_V is the "output" energy sensitivity [the output signal of a SQUID is $V(t)$], ϵ_I describes the intensity of backaction noise, and ϵ_{IV} characterizes their correlation. From the inequality $\epsilon_I \epsilon_V \geq \hbar^2/4$ we easily get an inequality for spectral densities: $s_I s_V \geq \hbar^2 (dV/d\Phi)^2$, where $dV/d\Phi$ describes the SQUID response to the flux Φ. For the two-SQUID measurement setup considered in the present paper the qubit dephasing due to backaction noise is $\Gamma_d = (\Delta\Phi)^2 s_I/4\hbar^2$ where $\Delta\Phi$ is the measured flux difference between two qubit states. Using the inequality above for the product $s_I s_V$ we obtain a lower bound for the ensemble decoherence rate: [48] $\Gamma_d \geq (\Delta V)^2/4s_V = (2\tau_m)^{-1}$ similar to all other setups discussed above. This lower bound can be achieved only when the SQUID sensitivity is quantum-limited.

Notice that the main equations (14)?(15) of the conventional formalism do not depend on the detector output $I(t)$, and so they cannot be used for the prediction of the detector current behavior [for generality we again choose the current as a detector output signal even though for a SQUID it should be changed to $V(t)$]. An important step towards this goal has been made in Ref. [39] for a tunnel junction as a detector (a similar analysis for the single-electron transistor has been performed in Refs. [50,62]). Let us divide the density matrix ρ_{ij} into terms corresponding to different numbers n of electrons passed through the measuring tunnel junction, $\rho_{ij} = \sum_n \rho_{ij}^n$ (only

10

diagonal terms in n are considered). Then the evolution of these terms is given by the equations [39]

$$\dot{\rho}_{11}^n = -\frac{I_1}{e}\rho_{11}^n + \frac{I_1}{e}\rho_{11}^{n-1} - 2\frac{H}{\hbar}\operatorname{Im}\rho_{12}^n \tag{22}$$

$$\dot{\rho}_{22}^n = -\frac{I_2}{e}\rho_{22}^n + \frac{I_2}{e}\rho_{22}^{n-1} + 2\frac{H}{\hbar}\operatorname{Im}\rho_{12}^n \tag{23}$$

$$\dot{\rho}_{12}^n = i\frac{\varepsilon}{\hbar}\rho_{12}^n + i\frac{H}{\hbar}(\rho_{11}^n - \rho_{22}^2) - \frac{I_1 + I_2}{2e}\rho_{12}^m \tag{24}$$

while Eqs. (14)-(15) can be derived from Eqs. (22)-(24) after summation over n.

Even though these equations couple the evolution of the system density matrix with the number of electrons passed through the detector, they cannot predict the behavior of the current $I(t)$ and do not allow the calculation of ρ_{ij} for a given realization of $I(t)$. Actually, this is quite expected since the conventional formalism describes the *ensemble averaged* evolution while the analysis of a particular measurement realization requires a formalism suitable for an *individual* quantum system. (The use of the conventional formalism was the reason why several recent attempts [45,62,63] to analyze the detector current were not very successful.) The analysis of a particular realization of the measurement process can be performed using the Bayesian formalism discussed in the next section.

4. Bayesian Formalism

In the Bayesian formalism (the name originates from the Bayes formula [64,65] for probabilities) which was derived only for the weakly responding (linear) regime, the evolution of the qubit density matrix during a particular measurement process is described by the equations [33]

$$\dot{\rho}_{11} = -\dot{\rho}_{22} = -2\frac{H}{\hbar}\operatorname{Im}\rho_{12} + \rho_{11}\rho_{22}\frac{2\Delta I}{S_0}[I(t) - I_0] \tag{25}$$

$$\dot{\rho}_{22} = i\frac{\varepsilon}{\hbar}\rho_{12} + i\frac{H}{\hbar}(\rho_{11} - \rho_{22}) - (\rho_{11} - \rho_{22})\frac{2\Delta I}{S_0}[I(t) - I_0]\rho_{12} - \gamma_d\rho_{12} \tag{26}$$

11

place Eqs. (14)-(15) of the conventional formalism. Here

$$\gamma_d = \Gamma_d - \frac{(\Delta I)^2}{4S_0} \geq 0 \tag{27}$$

is the decoherence rate due to the "pure environment" only (ideal continuous measurement does not lead to this decoherence). One can see that $\gamma_d = 0$ in the example of a tunnel junction as a detector, which thus can be called an ideal detector, $\eta = 1$, where

$$\eta \equiv 1 - \frac{\gamma_d}{\Gamma_d} = \frac{1}{2\Gamma_d \tau_m} \tag{28}$$

A similar ideal situation occurs for a quantum point contact when $\Gamma_d = (\Delta I)^2/4S_0$, and also for the two- SQUID setup when the sensitivity of the measuring SQUID is quantum-limited and the output and backaction noises are uncorrelated. The important prediction of the Bayesian formalism is that in such an ideal situation (which is experimentally accessible), an initially pure state of the qubit remains pure during the evolution; moreover, an initially mixed state can be gradually purified in the course of continuous measurement. [33]

Eqs. (25)-(26) allow us to calculate the evolution of ρ_{ij} for a given measurement output $I(t)$. In order to analyze the behavior of $I(t)$, these equations should be complemented by the formula

$$I(t) - I_0 = \frac{\Delta I}{2})\rho_{11} - \rho_{22}) + \xi(t) \tag{29}$$

where $\xi(t)$ is a zero-correlated ("white") random process with the same spectral density as the detector noise, [66] $S_\xi = S_0$. The stochasticity of the detector current does not allow us to predict exactly the evolution of ρ_{ij} in each particular realization of the measurement process; however, the formalism describes the mutual dependence of the stochastic evolutions of $\rho_{ij}(t)$ and $I(t)$ and thus allows us to make experimental predictions not accessible by the conventional approach.

When Eq. (29) is substituted into Eqs. (25)?(26), we get a system of nonlinear stochastic differential equations. The analysis of such equations requires special care, since their solution depends on the accepted definition of the derivative [67] (this happens because the noise increases with

12

the decrease of the timescale, and so $\overline{\xi^2 dt} = $ constant $= S_\xi/2$ does not decrease with dt). In Eqs. (25)-(26) we have used the symmetric definition, $\dot\rho(t) = \lim_{\tau\to 0}[\rho(t+\tau/2) - \rho(t-\tau/2)]/\tau$. This is the so-called Stratonovich interpretation of the nonlinear stochastic equations. The main advantage of this interpretation is that all standard calculus formulas [for example, $(fg)' = f'g + fg'$] remain valid, [67] so the intuition based on usual (non-stochastic) differential equations typically works well (this is the reason why we prefer the Stratonovich interpretation). Its other advantage is the correct limit in the case when the white noise term is approximated by a properly converging sequence of smooth functions. [67]

However, for some purposes (e.g., for averaging over stochastic variables and for numerical simulations) it is more convenient to use another definition of the derivative: $\dot\rho(t) = \lim_{\tau\to 0}[\rho(t+\tau) - \rho(t)]/\tau$. This is called the Itô interpretation and it is the most commonly used interpretation in mathematical literature on stochastic differential equations. There is a simple rule of translation between the two interpretations: [67] for an arbitrary system of equations

$$\dot x_i(t) = G_i(\mathbf{x}, t) + F_i(\mathbf{x}, t)\xi(t) \tag{30}$$

in Stratonovich interpretation, the corresponding Itô equation which has the same solution is

$$\dot x_i(t) = G_i(\mathbf{x}, t) + \frac{S_\xi}{2}\sum_k \frac{\partial F_i(\mathbf{x}, t)}{\partial x_k}F_k(\mathbf{x}, t) + F_i(\mathbf{x}, t)\xi(t) \tag{31}$$

where $x_i(t)$ are the components of the vector $\mathbf{x}(t)$, G_i and F_i are arbitrary functions, and the constant S_ξ is the spectral density of the white noise process $\xi(t)$. Applying this transformation to Eqs. (25), (26), and (29) we get the following equations in Itô interpretation:

$$\dot\rho_{11} = -\dot\rho_{22} = -2\frac{H}{\hbar}\operatorname{Im}\rho_{12} + \rho_{11}\rho_{22}\frac{2\Delta I}{S_0}\xi(t) \tag{32}$$

$$\dot\rho_{22} = i\frac{\varepsilon}{\hbar}\rho_{12} + i\frac{H}{\hbar}(\rho_{11} - \rho_{22}) - (\rho_{11} - \rho_{22})\frac{2\Delta I}{S_0}\rho_{12}\xi(t) - \left[\gamma_d + \frac{(\Delta I)^2}{4S_0}\right]\rho_{12} \tag{33}$$

while the current $I(t)$ is still given by Eq. (29). Similar equations (in a different notation) have been obtained in Ref. [27] for a symmetric two-level system measured by an ideal detector ($\varepsilon = 0, \gamma_d = 0$). Notice that the Itô interpretation has been used in the majority of theories describing selective

evolution due to quantum measurement (see [17-19] and references therein).

Using the Itô interpretation it is easier to see that averaging of the evolution equations over the random process $\xi(t)$ (i.e., averaging over different detector outputs) leads to the conventional equations (14)-(15). However, for the analysis of an individual realization of the evolution, Itô equations are typically less transparent for physical interpretation. For example, the term $-\rho_{12}(\Delta I)^2/4S_0$ in Eq. (33) does not actually cause decoherence in an individual realization but just compensates the noise term proportional to $\xi^2 dt$ due to the Itô definition of the derivative, and so $\rho_{12}(t)$ does not decrease exponentially in time if $H \neq 0$. Similarly, the fact that the measurement tries to localize the density matrix in one of two states is not clear from Eqs. (32)-(33) while it is obvious from Eqs. (25)-(29).

To avoid confusion due to the difference between Stratonovich and Itô interpretations, it is helpful to write the exact solution of Eqs. (25)-(26) [which is also the solution of Eqs. (32)-(33)] in the special case $H = 0$:

$$\frac{\rho_{11}(t+\tau)}{\rho_{22}(t+\tau)} = \frac{\rho_{11}(t)}{\rho_{22}(t)} \frac{\exp\left[-(\bar{I}(\tau) - I_1)^2 \tau/S_0\right]}{\exp\left[-(\bar{I}(\tau) - I_2)^2 \tau/S_0\right]} \tag{34}$$

$$\frac{\rho_{12}(t+\tau)}{[\rho_{11}(t+\tau)\rho_{22}(t+\tau)]^{1/2}} = \frac{\rho_{12}(t)e^{i\varepsilon\tau/\hbar}}{[\rho_{11}(t)\rho_{22}(t)]^{1/2}} e^{-\gamma_d \tau} \tag{35}$$

where

$$\bar{I}(\tau) \equiv \frac{1}{\tau} \int_t^{t+\tau} I(t')dt' \tag{36}$$

is the detector current averaged over the time interval $(t, t+\tau)$. These equations have clear physical meaning: Eq. (34) is just the Bayes formula (see next section) while Eq. (35) describes gradual decoherence due to the "pure environment" characterized by γ_d.

A useful tool for analysis of the measurement process is Monte-Carlo simulation of an individual process realization. For this purpose we can use Eqs. (34)-(35) complemented by the simulation of evolution due to finite H. Let us choose a sufficiently small timestep Δt (much smaller than $\hbar/H$) and apply the following algorithm. First, for each timestep $(t, t + \Delta t)$ we pick the averaged current

$$\bar{I} \equiv \frac{1}{\Delta t} \int_t^{t+\Delta t} I(t')dt'$$

14

as a random number using the probability distribution

$$P(\bar{I}) = \frac{\rho_{11}(t)}{2\pi D)^{1/2}} \exp\left[-\frac{(\bar{I} - I_1)^2}{2D}\right] + \frac{\rho_{22}(t)}{2\pi D)^{1/2}} \exp\left[-\frac{(\bar{I} - I_2)^2}{2D}\right] \quad (37)$$

where $D = S_0/2\Delta t$. Then $\bar{I}$ is substituted into Eqs. (34)-(35) to calculate $\rho_{ij}(t + \Delta t)$ from $\rho_{ij}(t)$. The last step of the procedure is the additional evolution during Δt due to finite H (rotation in the $\rho_{11} - \rho_{22}$ plane). Then the whole procedure is repeated for the next timestep Δt and so on.

An alternative algorithm can be based directly on the Itô equations (32)-(33) which are more natural for numerical simulations than the Stratonovich equations because of the "forward-looking" definition of the derivative. For sufficiently small Δt (now much smaller than all timescales $S_0/(\Delta I)^2, \hbar/H$, $\hbar/\varepsilon$, and γ_d^{-1}) we first calculate the averaged pure noise,

$$\bar{\xi} \equiv \frac{1}{\Delta t} \int_t^{t+\Delta t} \xi(t')dt'$$

as a random number using the Gaussian distribution

$$P(\bar{\xi}) = \frac{1}{(2\pi D)^{1/2}} \exp\left[-(\bar{\xi})^2/2D\right] \quad (38)$$

where again $D = S_0/2\Delta t$. Then this number is substituted into Eq. (32):

$$\rho_{11}(t + \Delta t) = \rho_{11}(t) - 2\Delta t \frac{H}{\hbar} \operatorname{Im} \rho_{12}(t) + \rho_{11}(t)\rho_{22}(t)\frac{2\Delta I}{S_0}\bar{\xi}\Delta t \quad (39)$$

and similarly into Eq. (33). Then the updating procedure is repeated for the next step Δt and so on. The detector current can be calculated using Eq. (29).

Both Monte-Carlo algorithms are equivalent; however, the first algorithm is better because it allows longer timesteps. The equivalence for small Δt can be proven analytically using a second-order series expansion of Eqs. (34)-(35) and has also been checked numerically. Notice that for $\Delta t \ll S_0/(\Delta I)^2$, the current distribution (37) is indistinguishable from the distribution $P(\bar{\xi} + \Delta I(\rho_{11} - \rho_{22})/2)$ given by Eq. (38).

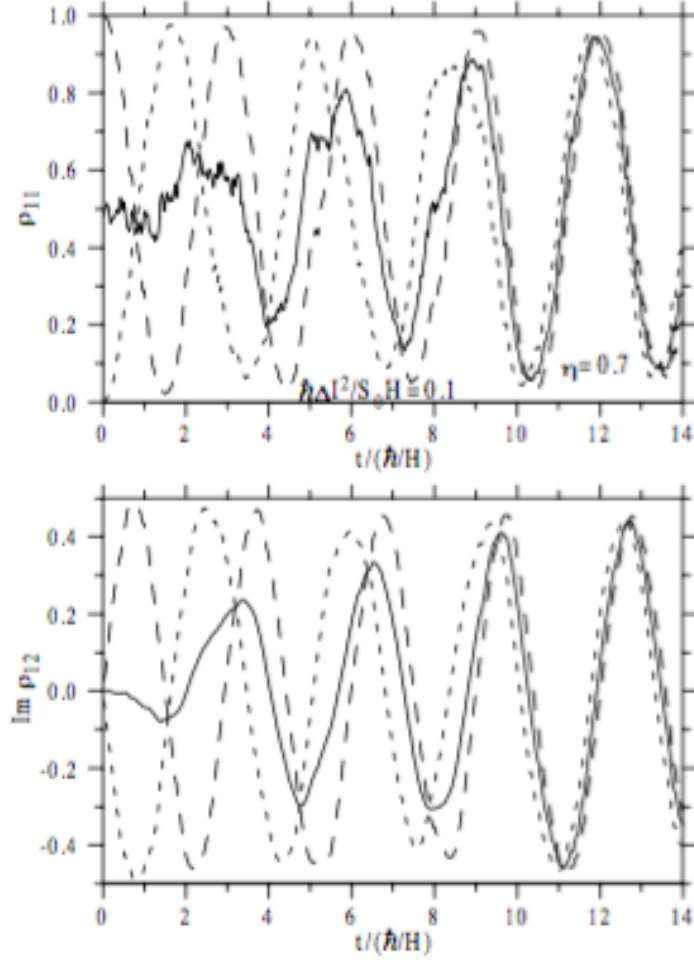A typical result of the Monte-Carlo simulation is shown in Fig. 3.

Figure 3: Solid lines: gradual purification of the qubit density matrix $\rho(t)$ in the course of continuous measurement, starting from the completely incoherent state. Dashed lines show the evolution starting from localized states, assuming the same detector current.

The solid lines show a particular realization of the evolution of $\rho(t)$ (diagonal and nondiagonal elements of the density matrix) for a symmetric qubit, $\varepsilon = 0$, measured by a detector with coupling $\mathcal{C} \equiv \hbar(\Delta I)^2/S_0 H = 0.1$ and ideality factor $\eta = 0.7$. The real part of $\rho_{12}(t)$ is not shown since its evolution is decoupled from $\rho_{11}(t)$ and $\mathrm{Im}\,\rho_{12}(t)$. The completely incoherent initial state is chosen, $\rho_{11}(0) = 0.5$, $\rho_{12}(0) = 0$. Nevertheless, the measurement leads to

16

the gradual onset of quantum coherent oscillations. This happens because the measurement randomly tries to localize the qubit, while the finite H provides oscillations when the state becomes at least partially localized. The qubit state is gradually purified, eventually reaching a pure state if the detector is ideal. For a nonideal detector (Fig. 3) the state remains partially incoherent, which decreases the amplitude of the oscillations.

The qubit gradually "forgets" its initial state during the evolution and the density matrix $\rho(t)$ becomes determined mostly by the detector record. To illustrate this fact, the dashed lines in Fig. 3 show the qubit evolution calculated by Eqs. (25)-(26) starting from two localized states and assuming that the detector current (not shown) is exactly the same as in the measurement realization corresponding to the solid lines. As expected, after the time comparable to τ_m the dashed lines become close to the solid lines.

The tendency to qubit state localization due to measurement can be described quantitatively using the deterministic part of Eqs. (25) and (29). However, because of the equation nonlinearity the typical localization time τ_l cannot have a unique definition. If we define it via an exponential-growth factor $\exp(t/\tau_l)$ for $\rho_{11}(t)$-evolution when ρ_{11} is close to $1/2$, then

$$\tau_l = 2\frac{S_0}{(\Delta I)^2} \tag{40}$$

which exactly coincides with the definition of the typical measurement time τ_m. [If for the definition we choose the exponential-decrease factor $\exp(t/\tau_l)$ when the state is almost localized, then τ_l would be twice smaller.]

5. Derivation Based on Bayes Formula

In this section we briefly review the derivation of the Bayesian formalism presented in Ref. [33], which was based on the correspondence between classical and quantum measurements.

In the classical case ($H = 0, \rho_{12} = 0$) the measurement process can be described as an evolution of probabilities ρ_{11} and ρ_{22} which reflect our knowledge about the system state. Then for arbitrary Δt (which can be comparable to τ_m) the average current $\bar{I}$ obviously has the probability distribution given

17

by Eq. (37). After the measurement during Δt the information about the system state has increased and the probabilities ρ_{11} and ρ_{22} should be updated using the measurement result $\bar{I}$ and the Bayes formula (34), which completely describes the classical measurement. [The Bayes formula [64,65] says that the updated probability $P^*(\mathcal{A})$ of a hypothesis $\mathcal{A}$ given that event $\mathcal{F}$ has ??happened in an experiment, is equal to

$$P^*(\mathcal{A}) = \frac{P(\mathcal{A})P(\mathcal{F}|\mathcal{A})}{\sum_{\mathcal{B}}[P(\mathcal{B})P(\mathcal{F}|\mathcal{B})]}$$

where $P(\mathcal{A})$ is the probability before the experiment, $P(\mathcal{F}|\mathcal{A})$ is the conditional probability of event $\mathcal{F}$ for hypothesis $\mathcal{A}$, and the sum is over the complete set of mutually exclusive hypotheses.]

The next step is an important assumption: in the quantum case with $H = 0$ the evolution of ρ_{11} and ρ_{22} is still given by Eq. (34) because there is no principal possibility to distinguish between classical and quantum cases, performing only this kind of measurement. Even though this assumption is quite obvious, it is not derived formally but should rather be regarded as a consequence of the correspondence principle. In other words, this is the natural generalization of the collapse postulate to the case of incomplete measurement.

The comparison with classical measurement cannot de- scribe the evolution of ρ_{12}; however, there is an upper limit: $|\rho_{12}| \leq [\rho_{11}\rho_{22}]^{1/2}$. Surprisingly, this inequality is sufficient for the exact calculation of $\rho_{12}(t)$ in the important special case of an ideal detector and $H = 0$. Averaging this inequality over all possible detector outputs $\bar{I}$ using distribution (37) we get the inequality

$$|\rho_{12}(t+\tau)| \leq [\rho_{11}\rho_{22}]^{1/2} \exp\left[-\frac{(\Delta I)^2}{4S_0}\tau\right] \tag{41}$$

On the other hand, for such averaged dynamics Eq. (41) actually reaches the upper bound [see Eqs. (14)-(15) and (18)] in the cases discussed in Section 3 (tunnel junction, symmetric quantum point contact, or quantum-limited SQUID as a detector). This is possible *only* if in each realization of the measurement process the initially pure density matrix $\rho_{ij}(t)$ stays pure all the time, $\|\rho_{12}(t)\|^2 = \rho_{11}(t)\rho_{22}(t)$. This fact has been the main point in the Bayesian formalism derivation in Ref.[33].

As the next step of the derivation, a mixed initial state has been taken into account (for $H = 0$ and an ideal detector) using conservation of the "degree of purity" [Eq. (35) with $\gamma_d = 0$] which directly follows from a statistical consideration. The qubit state evolution due to finite H has been simply added to the evolution due to measurement. Finally, the interaction with the extra environment (which does not provide any measurement result) has been taken into account by introducing the decoherence rate γ_d.

First-order series expansion of the corresponding equations for $\rho_{ij}(t + \Delta t)$ leads to differential equations (25)? (26). The reason why we get equations in Stratonovich interpretation is that the first-order expansion is necessarily based on the standard calculus rules which are valid only in this interpretation. Using a second-order expansion we can obtain differential equations both in Stratonovich and Itô interpretations, depending on the definition of the derivative.

6. Alternative Derivation of the Formalism

Let us discuss now an alternative way of deriving the Bayesian formalism, which is based on Eqs. (22)-(24) of the conventional approach (a somewhat similar derivation of the Bayesian formalism has been recently presented in Ref. [36]). Since these equations have been derived [39] only for the tunnel junction as a detector, we limit ourselves to this case.

Eqs. (22)-(24) describe the coupled evolution of the qubit density matrix ρ_{ij} and the number n of electrons passed through the detector, considering the "qubit plus detector" as a closed system. We need to make a small but very important step in order to describe an individ- ual measurement process: we need to construct an open system which outputs classical information to the out- side. For this purpose let us introduce the next stage of the measurement setup which will be called "pointer" (see Fig. 4). By definition, the pointer deals only with classical signals while quantum description is allowed for the detector.
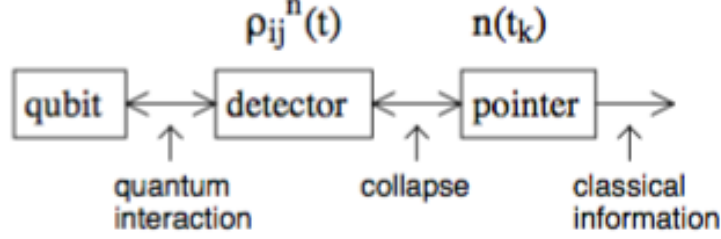
Figure 4: The pointer is introduced into the model to ex- tract the classical signal from the detector.

Let us consider the following model. The pointer does not interact with the detector most of the time, however, at time moments $t = t_k$ $(k = 1, 2, ...)$ the pointer measures (in simple orthodox way) the total number n of electrons passed through the detector. By our assumption the measured n should be a classical number, so after each measurement by the pointer the number $n_k = n(t_k)$ is well defined. However, during the "free" evolution of the "qubit plus detector" between the measurements by pointer the number $n(t)$ gets smeared according to Schrödinger equation, i.e., satisfy Eqs. (22)-(24). By introducing sufficiently frequent readout (collapse) into the model we get the ability to describe the time dependence of the detector current. Of course, many other collapse scenarios are possible, however, if we show that within some limits the measurement process does not depend on the choice of times t_k, this is a good argument justifying the generality of the model.

The collapse at $t = t_k$ can be described in the orthodox way. [10-12] The probability $P(n)$ to measure n electrons passed through a detector is

$$P(n) = \rho_{11}^n(t_k) + \rho_{22}^n(t_k) \tag{42}$$

The measurement by pointer picks some random number n_k according to distribution (42), however, after the measurement this number is already well defined and the density matrix should be immediately updated (collapsed): [10?12]

$$\rho_{ij}^n(t_k + 0) = \delta_{n,n_k} \rho_{ij}(t_k + 0) \tag{43}$$

$$\rho_{ij}(t_k + 0) = \frac{\rho_{ij}^{n_k}(t_k - 0)}{\rho_{11}^{n_k}(t_k - 0) + \rho_{22}^{n_k}(t_k - 0)} \tag{44}$$

20

where δ_{n,n_k} is the Kronecker symbol. After that the evolution is described by Eqs. (22)-(24) until the next collapse occurs at $t = t_{k+1}$.

The detector current in our model has a natural averaging during time period between t_{k-1} and t_k and can be calculated as

$$\bar{I}_k = \frac{e\Delta n_k}{\Delta t_k}$$

where $\Delta n_k \equiv n(t_k) - n(t_{k-1})$ and $\Delta t_k \equiv t_k - t_{k-1}$. Since the detector output is intended to reflect the evolution of the measured system, t_k should be sufficiently frequent, in particular $\Delta t_k \hbar/H$. For a while let us completely neglect the terms proportional to H in Eqs. (22)-(24) and discuss their effect later. Then these equations can be solved exactly. For the initial condition $\rho_{ij}^n(0) = \delta_{n,0}\rho_{ij}(0)$ the solution is

$$\rho_{11}^n(t) = \frac{(I_1 r/e)^n}{n!} \exp\left(-I_1 t/e\right)\rho_{11}(0) \tag{45}$$

$$\rho_{22}^n(t) = \frac{(I_2 r/e)^n}{n!} \exp\left(-I_2 t/e\right)\rho_{22}(0) \tag{46}$$

$$\rho_{12}^n(t) = \frac{(\sqrt{I_1 I_2}/e)^n}{n!} \exp\left(-\frac{I_1 + I_2}{2e}t + \frac{i\varepsilon t}{\hbar}\right)\rho_{12}(0) \tag{47}$$

Similar equations describe the evolution after kth measurement by the pointer, just t is shifted by t_k and n is shifted by n_k. Using Eqs. (43)-(44) we derive the iterative equations for the qubit density matrix:

$$\begin{aligned}
\rho_{11}(t_k) = {} &\rho_{11}(t_{k-1})I_1^{\Delta n_k} \exp\left(-I_1\Delta t_k/e\right) \\
&\times \left[\rho_{11}(t_{k-1})I_1^{\Delta n_k} \exp\left(-I_1\Delta t_k/e\right)\right. \\
&\left. + \rho_{22}(t_{k-1})I_2^{\Delta n_k} \exp\left(-I_2\Delta t_k/e\right)\right]^{-1}
\end{aligned} \tag{48}$$

$$\rho_{22}(t_k) = 1 - \rho_{11}(t_k) \tag{49}$$

$$\rho_{12}(t_k) = \rho_{12}(t_{k-1})\left[\frac{\rho_{11}(t_k)\rho_{22}(t_k)}{\rho_{11}(t_{k-1})\rho_{22}(t_{k-1})}\right]^{1/2} \exp\left(i\varepsilon\Delta t_k/\hbar\right) \tag{50}$$

while the probability $P(n_k)$ to get $n = n_k$ at $t = t_k$ is

$$\begin{aligned}
P(n_k) = {} &\frac{(\Delta t_k/e)^{\Delta n_k}}{(\Delta n_k)!}\left[I_1^{\Delta n_k} \exp\left(-I_1\Delta t_k/e\right)\rho_{11}(t_{k-1})\right. \\
&\left. + I_2 1^{\Delta n_k} \exp\left(-I_2\Delta t_k/e\right)\rho_{22}(t_{k-1})\right]
\end{aligned} \tag{51}$$

It is instructive to check that the averaging of $\rho_{ij}(t_k)$ over the result of measurement at $t = t_k$ gives simple equations

$$\overline{\rho_{11}(t_k)} = \rho_{11}(t_{k-1}) \quad , \quad \overline{\rho_{22}(t_k)} = \rho_{22}(t_{k-1}) \tag{52}$$

$$\overline{\rho_{12}(t_k)} = \rho_{12}(t_{k-1}) \exp\left(i\varepsilon\Delta t_k/\hbar\right) \exp\left[-(\sqrt{I_1} - \sqrt{I_2})^2 \Delta t_k/2e\right] \tag{53}$$

which are consistent with the conventional equations (14)-(16). [68]

One can easily see that Eq. (48) can be interpreted as the Bayes formula, while Eq. (50) is the conservation of the "degree of purity", similar to the approach reviewed above. The complete equivalence between Eqs. (48)-(51) and Eqs. (34)-(37) is achieved if $|\Delta I| \ll I_0$ and also the probing time Δt_k is much longer than the typical time I_0/e between individual electron passages in the detector (so that the current is essentially continuous). In this case the Poissonian distributions (45)-(46) obviously become Gaussian, and so the probability distributions for the current $\bar{I} = e\Delta n_k/\Delta t_k$ given by Eq. (37) and Eq. (51) coincide. Similarly, Eqs. (48)-(50) for ρ_{ij} coincide with Eqs. (34)-(35) applied to an ideal detector,$\gamma_d = 0$. [69]

If the probing period is within the range $e/I_0 \ll \Delta t_k \ll eI_0/(\Delta I)^2$, the evolution of ρ_{ij} is smooth and so Eqs. (48)-(49) can be written in a differential form which coincides with Eqs. (25)-(26) of the Bayesian formalism with $H = 0$ and $\gamma_d = 0$. The effect of finite H can be now taken into account by the addition of obvious terms into Eqs. (25)-(26). However, this can be done only if $\Delta t_k \ll H/\hbar$ because in the opposite case the terms of more than the first power in H should be added into Eqs. (48)-(50) indicating a nontrivial interplay between two effects.

So, we have shown that in the weakly responding case, $\Delta I \ll I_0$, Eqs. (22)-(24) of the conventional approach complemented by a sufficiently frequent readout (collapse), $e/I_0 \ll \Delta t_k \ll \min[eI_0/(\Delta I)^2, \hbar/H]$ lead to the equations of the Bayesian approach. The decoherence rate γ_d is zero because the model39 describes a tunnel junction which is an ideal detector.

7. Effect of Collapse Due to Pointer

The simple model considered in the previous section allows us to analyze the effect of the repeated measurements by pointer on the qubit dynamics in

more detail and beyond the approximations of the Bayesian approach. First, it is important to notice that in this model the event of collapse at $t = t_k$ does not disturb the qubit measurement by the detector. More specifically, the collapse with unknown result n_k is equivalent to the absence of the collapse. To prove this fact, Eqs. (43)-(44) can be averaged with the distribution (42) that results in unity operator.

The absence of disturbance by pointer is because in the model there are no density matrix elements which couple detector states with different number of passed electrons. Physically, this is a consequence of the assumption of low detector barrier transparency and infinite number of electrons in the detector electrodes, so that the "attempt frequency" is much larger than any collapse frequency (for a quantum point contact the necessary condition for this assumption is the large resistance, $R \gg \hbar/e^2$). In other words, this model is intrinsically Markovian and the detector is classical in a sense that the passage of individual electrons through detector is essentially classical (not quantum) random process. [70]

The absence of the disturbance by collapse with un- known result does not mean, however, that we can forget about the collapse and make it only "at the end of the day". Any readout from the detector necessarily changes the qubit state (or in other words, informs us about the change) and thus affects the qubit evolution. In the limit of sufficiently often readout, $\Delta t_k \ll \min(e/I_1, e/I_23, \hbar/H, \hbar/\varepsilon)$, the evolution equations (22)-(24) and (42)-(44) simplify because at most one electron can pass through the detector between readouts. During the periods of time when no electrons are passed through the detector, the evolution is essentially described by Eqs. (22)-(24) with $n = 0$, while the frequent collapses just restore the density matrix normalization, leading to the continuous qubit evolution:

$$\dot{\rho}_{11} = -\dot{\rho}_{22} = -1\frac{H}{\hbar}\operatorname{Im}\rho_{12} - \frac{\Delta I}{e}\rho_{11}\rho_{22} \tag{54}$$

$$\dot{\rho}_{12} = \frac{i\varepsilon}{\hbar}\rho_{12} + \frac{iH}{\hbar}(\rho_{11} - \rho_{22}) + \frac{\Delta I}{2e}(\rho_{11} - \rho_{22})\rho_{12} \tag{55}$$

However, at moments when one electron passes through the detector, the qubit state changes abruptly; this change is given by Eqs. (48)-(50) with $\Delta n_k = 1$ and $\Delta t_k \to 0$:

$$\rho_{11}(t + 0) = \frac{I_1\rho_{11}(t - 0)}{I_1\rho_{11}(t - 0) + I_2\rho_{22}(t - 0)} \tag{56}$$

$$\rho_{22}(t+0) = 1 - \rho_{11}(t+0) \tag{57}$$

$$\rho_{12}(t+0) = \rho_{12}(t-0)\left[\frac{\rho_{11}(t+0)\rho_{22}(t+0)}{\rho_{11}(t-0)\rho_{22}(t-0)}\right]^{1/2} \tag{58}$$

and can be obviously interpreted as the Bayesian update. Equations (54)-(58) correspond to the framework of "quantum jump" model. [18,36]

It is easy to see that initially pure qubit state remains pure under quantum jump evolution (54)-(58) and the density matrix is gradually purified if started from a mixed state. The lines in Fig. 5 show a particular realization of such evolution for $I_1/e = H/\hbar$, $I_1/I_2 = 3$, and completely incoherent initial state, $\rho_{11}(0) = 0.5$, $\rho_{112}(0) = 0$.
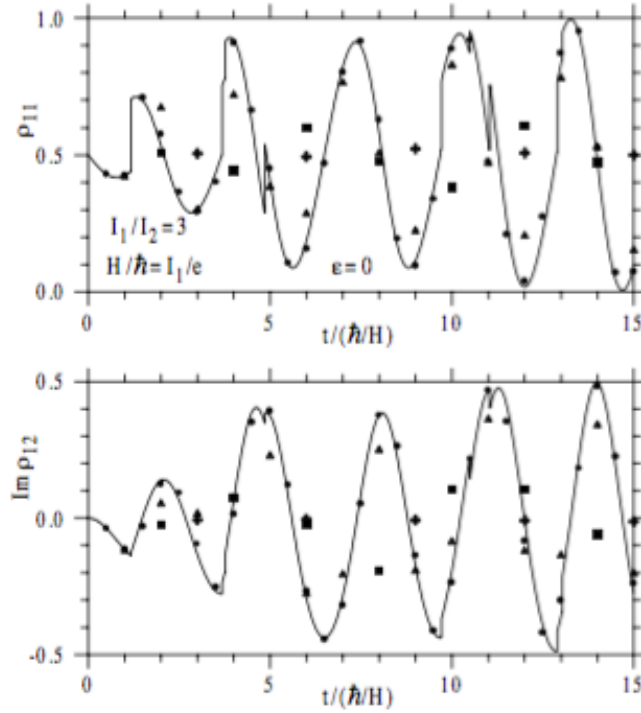

Figure 5: The lines show a gradual purification of the qubit density matrix $\rho(t)$ in the regime of quantum jumps (frequent detector readout with one-electron accuracy). The dots, triangles, squares, and crosses correspond to finite readout periods $\Delta t_k/(\hbar/H) = 0.5, 1, 2$ and 3 respectively.

24

Each discontinuity of curves corresponds to the passage of an electron through the detector (the jumps of ρ_{12} are typically smaller than the jumps of ρ_{11}). The matrix element ρ_{11} always jumps up because $I_1 > I_2$ and so the electron passage indicates that the state $|1\rangle$ is somewhat more likely than state $|2\rangle$. The jumps are more pronounced when ρ_{11} is closer to 0.5 because the jump amplitude is $\Delta\rho_{11} = \Delta I \rho_{11}\rho_{22}/(I_1\rho_{11} + I_2\rho_{22})$ [see Eq. (56)]. The model allows us to consider finite ratio I_1/I_2 in contrast to Eqs. (25)-(26) of the Bayesian approach. In the limit of weakly responding detector, $|\Delta I| \ll I_0$, the amplitude of quantum jumps (54)-(56) is negligible and Eqs. (25)-(26) are restored (in this sense they describe a "quantum diffusion" model [36]). Notice, however, that equations of the Bayesian approach are applicable to a broader class of detectors.

Since the model (22)-(24) describes the ideal detector, the qubit state in Fig. 5 eventually becomes completely pure. However, if the readout period Δt_k is not sufficiently small, the information about the moments of electron passage through the detector is partially lost that decreases our knowledge about the qubit state. In the formalism this leads to a partial decoherence of the qubit density matrix. The symbols in Fig. 5 (dots, triangles, squares, and crosses) represent the readout with several different periods for exactly the same realization of a measurement process as for the lines which represent very frequent readout. When the readout is still sufficiently frequent (dots), we can monitor the qubit evolution with a good accuracy (dots almost coincide with the lines). However, with the increase of the readout period, ρ_{11} becomes close to 0.5 and ρ_{12} becomes close to zero, indicating a strongly mixed state. Figure 6 shows the corresponding decrease of the average coherence factor $\theta \equiv 1 = 4\langle \rho_{11}\rho_{22} - |\rho_{12}|^2\rangle$ with increase of the readout period Δt_k (equal time between readouts is assumed). The averaging is done over the readout moments for sufficiently long realization of the measurement process. We also tried few other expressions which describe the density matrix coherence, all of them show a similar dependence on Δt_k. Notice the vanishing coherence in Fig. 6 when the ratio between Δt_k and the quantum oscillation period $\pi\hbar/H$ is close to an integer number (the regime of quantum nondemolition measurements [3,31]).
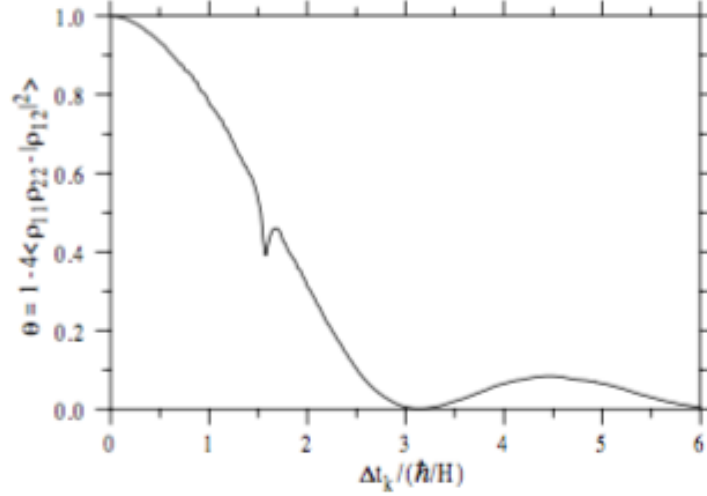
Figure 6: The average qubit coherence factor θ as a function of the readout period Δt_k for the measurement process shown in Fig. 5.

In the special case $H = 0$ all the information about the qubit state is contained in the result of the last measurement by pointer. This fact can be easily proven by applying Eqs. (48)-(50) twice and checking that resulting qubit density matrix does not depend on the result n_1 of the first measurement while the dependence on the second result n_2 is the same as in the case of only one last measurement. Similarly, the probability distribution $P(n_2)$ [see Eq. (51)] averaged over the result n_1 of the first measurement exactly coincides with $P(n_2)$ in absence of the first measurement.

It is interesting to discuss the generalization of the model to the case of a low-transparency tunnel junction with finite temperature of electrodes. Then each of the currents I_1 and I_2 can be decomposed into two currents flowing in opposite directions,

$$I + i = I_i^+ - I_i^- \quad , \quad \frac{I_i^+}{I_i^-} = \beta eV \tag{59}$$

where $i = 1, 2, 3$, $beta$ is the inverse temperature, and V is the voltage across junction. In this case Eqs. (22)-(24) are replaced by the following equations:

$$\dot{\rho}_{11}^n = -\frac{I_1^+ + I_1^-}{e}\rho_{11}^n + \frac{I_1^+}{e}\rho_{11}^{n-1} + \frac{I_1^-}{e}\rho_{11}^{n+1} - 2\frac{H}{\hbar}\text{Im}\,\rho_{12}^n \tag{60}$$

26

$$\dot{\rho}_{22}^n = -\frac{I_2^+ + I_2^-}{e}\rho_{22}^n + \frac{I_2^+}{e}\rho_{22}^{n-1} + \frac{I_2^-}{e}\rho_{22}^{n+1} + 2\frac{H}{\hbar}\text{Im}\,\rho_{12}^n \tag{61}$$

$$\dot{\rho}_{12}^n = i\frac{\varepsilon}{\hbar}\rho_{12}^n + i\frac{H}{\hbar}(\rho_{11}^n - \rho_{22}^n) - \frac{I_1^+ + I_1^- + I_2^+ + I_2^-}{2e}\rho_{12}^n$$
$$+ \frac{\sqrt{I_1^+ I_2^+}}{e}\rho_{12}^{n-1} + \frac{\sqrt{I_1^- I_2^-}}{e}\rho_{12}^{n+1} \tag{62}$$

If the readout period Δt_k is much shorter than $\min(e/I_i^\pm, \hbar/H)$, the detector still does not decrease the qubit coherence in spite of the finite temperature. However, if individual electron passages are not resolved, the information about the number of electrons passed in each direction is lost that leads to the qubit decoherence. In the framework of Bayesian formalism in the case of quasi-continuous current, $e/I_i^\pm \ll \Delta t_k \ll \min[eI_i/(\Delta I)^2, \hbar/H)]$, we can easily calculate the output current noise $\Gamma_d = \coth(\beta eV/2)(\Delta I)^2/8eI_0$ (see also the derivation in Ref. [36]). Thus calculated detector ideality factor,

$$\eta = [\tanh(\beta eV/2)]^2 \tag{63}$$

becomes significantly less than unity at temperatures $\beta^{-1} \gtrsim eV$.

8. Detector with Correlated Output and Back-action Noises

Let us assume again a weakly responding (linear) detector and consider the case when the output detector noise is correlated with the "backaction" noise which provides the fluctuations $\varepsilon(t)$ of the qubit energy level difference and thus leads to the qubit dephasing. For example, this is the typical situation for a single-electron transistor as a detector. [54,55] In this case the knowledge of the noisy detector output $I(t)$ gives some information about the probable backaction noise "trajectory" $\varepsilon(t)$ which can be used to improve our knowledge of the qubit state. The compensation for the most probable trajectory $\varepsilon(t)$ leads to improved Bayesian evolution equations: [35]

$$\dot{\rho}_{11} = -\dot{\rho}_{22} = -2\frac{H}{\hbar}\text{Im}\,\rho_{12} + \rho_{11}\rho_{22}\frac{2\Delta I}{S_0}[I(t) - I_0] \tag{64}$$

$$\dot{\rho}_{12} = i\frac{\varepsilon}{\hbar}\rho_{12} + i\frac{H}{\hbar}(\rho_{11} - \rho_{22})$$
$$- (\rho_{11} - \rho_{22})\frac{2\Delta I}{S_0}[I(t) - I_0]\rho_{12}$$
$$+ iK[I(t) - (\rho_{11}I_1 + \rho_{22}I_2)]\rho_{12} - \tilde{\gamma}_d\rho_{12} \qquad (65)$$

where $K = (d\varepsilon/d\varphi)S_{I\varphi}/S_0\hbar$ characterizes the correlation between the noise of current I through the single-electron transistor and the noise of its central electrode potential φ ($S_{I\varphi}$ is the mutual low-frequency spectral density). [71] The term in square brackets after K in Eq. (65) is just the "pure output noise" from Eq. (29). The decoherence rate $-\tilde{\gamma}_d$ in Eq. (65) is now decreased because of partial recovery of the dephasing:

$$\tilde{\gamma}_d = \Gamma_d - \frac{(\Delta I)^2}{4S_0} - \frac{K^2 S_0}{4} \qquad (66)$$

The term containing K in Eq. (65) is proportional to the average $\varphi(t)$ for given $I(t)$. Performing ensemble averaging of this term [essentially, considering noise $\varphi(t)$ as uncorrelated with $I(t)$], we can reduce Eqs. (64)-(65) to Eqs. (25)-(26), while additional ensemble averaging over $I(t)$ leads to the conventional equations (14)-(15).

The obvious inequality $\tilde{\gamma}_d \geq 0$ (in the opposite case the condition $|\rho_{12}|^2 \leq \rho_{11}\rho_{22}$ would be violated) imposes a lower bound for the ensemble decoherence rate Γ_d:

$$\Gamma_d \geq \frac{(\Delta I)^2}{4S_0} + \frac{K^2 S_0}{4} \qquad (67)$$

which is stronger than the inequality $2\Gamma_d\tau_m \geq 1$ (see Section 3).

Inequality (67) can be also interpreted in terms of the energy sensitivity of a single-electron transistor. Let us define the output energy sensitivity as $\epsilon_I \equiv (dI/dq)^{-2}S_0/2C$ where C is the total island capacitance and dI/dq is the response to the externally induced charge q. Similarly, let us characterize the backaction noise intensity by $\epsilon_\varphi \equiv CS_{-}|varphi/2$ and the correlation between two noises by the magnitude $\epsilon_{I\varphi} \equiv (dI/dq)^{-2}S_{I\varphi}/2C$. Since in absence of other decoherence sources $\Gamma_d = S_\varphi(C\Delta E/2e\hbar)^2$, where ΔE is the energy coupling between qubit and single-electron transistor (see Section 3), and using also the reciprocity property $\Delta q = C\Delta E/e = d\varepsilon/d\varphi$, we can rewrite Eq. (67) as

$$\left(\epsilon_I\epsilon_\varphi - \epsilon_{I\varphi}^2\right)^{1/2} \geq \frac{\hbar}{2} \qquad (68)$$

similar to the result of Ref. [61] (see also Refs. [48,72-74]). When the limit $\hbar/2$ is achieved, the decoherence rate

$$\tilde{\gamma}_d = \frac{(\Delta I)^2}{4S_0}\left[\frac{\epsilon_I\epsilon_\varphi - \epsilon_{I_\varphi}^2}{(\hbar/2)^2} - 1\right] \tag{69}$$

in equations (64)-(65) for the selective evolution of an individual qubit vanishes, $\tilde{\gamma}_d = 0$. In this sense the detector is ideal, $\tilde{\eta} = 1$, where

$$\tilde{\eta} \equiv 1 - \frac{\tilde{\gamma}_d}{\Gamma_d} = \frac{\hbar^2(dI/dq)^2}{S_0 S_\varphi} + \frac{(S_{I_\varphi})^2}{S_0 S_\varphi} \tag{70}$$

even though it can be a nonideal detector $(\eta < 1)$ by the previous definition, $\eta = \hbar^2(dI/dq)^2/S_0 S_\varphi$. [Notice a simple relation,

$$\eta = \tilde{\eta} = \frac{(\hbar/2)^2}{\epsilon_I\epsilon_\varphi} = \frac{1}{2\Gamma_d\tau_m} \tag{71}$$

in absence of correlation between noises of $\varphi(t)$ and $I(t)$, $(S_{I_\varphi})^2 \ll S_0 S_\varphi$].

A similar conclusion is also valid for other kinds of detectors: a quantum-limited total energy sensitivity $\hbar/2$ is equivalent to detector ideality, $\tilde{\eta} = 1$. Besides the tunnel junction, [39] quantum point contact, [43,47] and SQUID, [61] the regime of ideal quantum detection is also achievable by superconducting single-electron transisitor [72] and normal single-electron transistor in cotunneling mode. [74] (The resonant-tunneling single-electron transistor [73] has ideality factor comparable, but not equal to unity.)

9. Quantum Feedback Loop

The Bayesian formalism allows us to monitor the evolution of an individual qubit using weak continuous measurement, thus avoiding strong instantaneous perturbations. This information can be used to control the qubit parameters ε and H in order to tune continuously the qubit state in such a way that the evolution follows the desired trajectory (a similar idea has been discussed in Refs. [30,34]). This is possible even in the presence of decoherence due to the environment and so presents an opportunity to suppress such decoherence.

Continuous qubit purification using a quantum feedback loop [38] can be useful for a quantum computer. All quantum algorithms require the supply of "fresh" qubits with well-defined initial states. This supply is not a trivial problem since a qubit left alone for some time deteriorates due to interaction with the environment. The usual idea is to use the ground state which should be eventually reached and does not deteriorate. However, to speed up the qubit initialization we need to increase the coupling with environment, which should be avoided. Another possible idea is to perform a projective measurement, after which the state becomes well-defined. However, in the realistic case the coupling with the detector is finite, which makes projective measurement impossible. So, a different idea is helpful: to tune the qubit continuously in order to overcome the dephasing due to the environment and so keep the qubit "fresh".

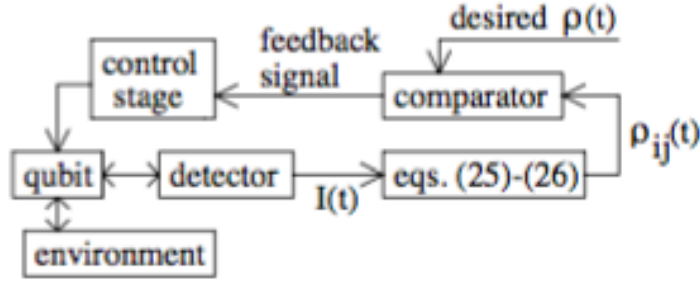The schematic of such state purification is shown in Fig. 7.

Figure 7: Schematic of continuous qubit purification using quantum feedback loop.

The qubit is continuously measured by a weakly coupled detector, and the detector signal is plugged into Eqs. (64)-(65) [or into Eqs. (25)-(26) in a simpler case] to monitor the evolution of the qubit density matrix $\rho_{ij}(t)$. This evolution is compared with the desired evolution, and the difference is used to generate the feedback signal which controls the qubit parameters H and ε in order to reduce the difference with the desired qubit state.

We have simulated a feedback loop designed to maintain the perfect quantum oscillations of a symmetric qubit $(\varepsilon = 0)$, so that the desired evolution is

$$\rho_{11} = \frac{1 + \cos{(\Omega t)}}{2} \quad , \quad \rho_{12} = \frac{i \sin{(\Omega t)}}{2}$$

30

where $\Omega = 2H/\hbar$. Let us assume an ideal detector, $\eta = 1$, so that the qubit decoherence rate γ_d in Eqs. (25)-(26) is due to the extra environment. The ratio between the decoherence rate and the "measurement rate" $(\Delta I)^2/4S_0$ is described by the factor $d \equiv 4S_0\gamma_d/(\Delta I)^2$.

To imitate a realistic situation the current $I(t)$ is averaged with a rectangular window of duration τ_a running in time, before it is plugged into Eqs. (25)-(26). So, thus calculated density matrix $\rho^a(t)$ differs (a little) from the "true" density matrix $\rho(t)$ which is simultaneously simulated by the Monte-Carlo method described in Section 4. The feedback signal is proportional to the difference $\Delta\phi$ between the desired oscillation phase $\Omega(t-\tau_a/2)$ and the phase calculated as

$$\phi(t) \equiv \tan^{-1}\left[\frac{2\mathrm{Im}\,\rho_{12}^1(t)}{\rho_{11}^a(t) - \rho_{22}^a(t)}\right]$$

Here the time shift $\tau_a/2$ partially compensates the detector signal delay due to averaging. The feedback signal is used to control the qubit tunnel barrier: $H_{fb}(t) = H[1 - F \times \Delta\phi(t - \tau_d)]$ where F is the dimensionless strength of the feedback and τ_d is an additional time delay ($\tau_d = 0$ is preferable but not achievable in a realistic situation).

Figure 8 shows typical realizations of the qubit's ρ_{11} evolution for

$$\mathcal{C} = \hbar(\Delta I)^2/S_0H = 1, \varepsilon = 0, \tau_a = 0.1\hbar/H, \tau_d = 0.05\hbar/H$$

and several values of the feedback factor $F = 0, 0.3$ and 3. No extra environment is assumed, $d = 0$. The qubit evolution starts from a localized state: $\rho_{11}(0) = 1$, $\rho_{12}(0) = 0$, and the desired evolution is shown by the thick solid line. Without a feedback ($F = 0$) the phase of quantum oscillations randomly fluctuates (diffuses) in time. However, for sufficiently large F the feedback "locks" the qubit evolution and makes it close to the desired one. Further increase of F decreases the difference between the actual and desired evolution. When F is too strong, the feedback loop becomes unstable. Overall, the behavior of this quantum feedback loop is similar to the behavior of a traditional classical feedback loop. In particular, we have checked that the increase of the averaging time τ_a and/or delay time τ_d eventually leads to synchronization breakdown. A decrease of the detector coupling $\mathcal{C}$ decreases the evolution disturbance due to measurement and allows more accurate tuning of quantum oscillations; on the other hand, in this case the feedback control becomes weaker and slower.
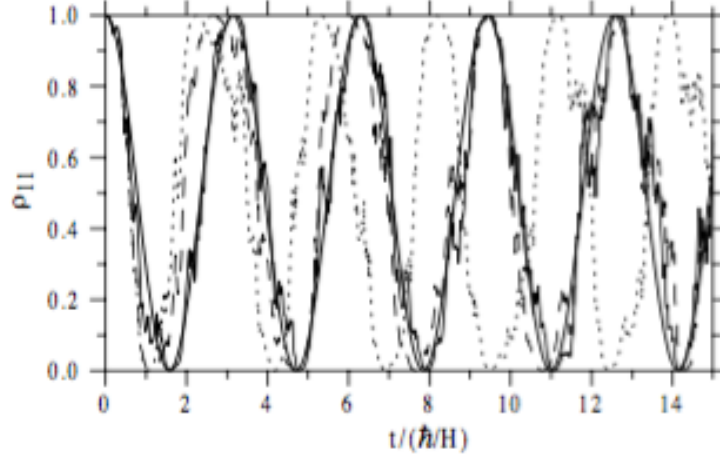
Figure 8: Particular realizations of the qubit evolution for a quantum feedback loop with strength $F = 3, 0.3$, and 0 (thin solid, dashed, and dotted lines, respectively). Thick line shows the desired evolution. No extra environment is present, $d = 0$.
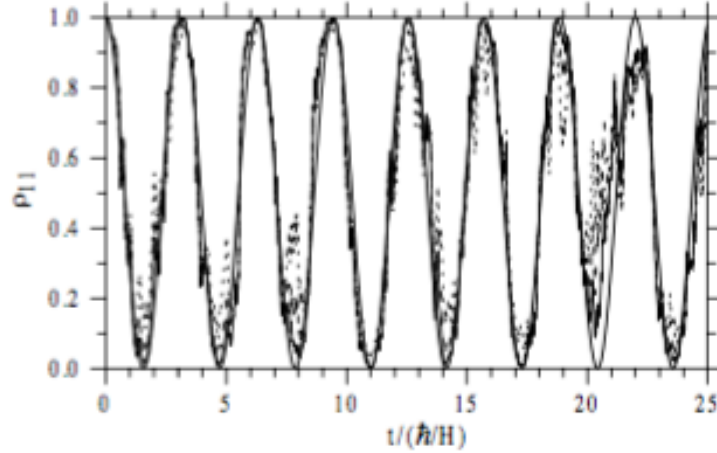

Figure 9: Operation of the quantum feedback loop (partic- ular realization) for several decoherence rates due to extra environment, $d = \gamma_d \times 4S_0/(\Delta I)^2 = 0.3, 1$ and 3 (thin solid, dashed, and dotted lines, respectively). Thick solid line is the desired evolution. $F = 3$, $\hbar(\Delta I)^2/S_0 H = 1$, $\varepsilon = 0$, $\tau_a = 0.1\hbar/H$, $\tau_d = 0.05\hbar/H$.

Qubit decoherence due to the presence of an extra environment prevents complete purification of the quantum oscillations so that the average qubit

coherence factor θ becomes less than 100%. However, if the qubit coupling with the detector is stronger than the coupling with its environment, $d \lesssim 1$, the feedback loop still provides qubit evolution quite close to the desired one (see Fig. 9). Most noticeably, the phase of quantum oscillations does not diffuse far from the desired value Ωt. So, for example, the spectral density of these oscillations has a delta-function shape at frequency Ω (with exponentially small width) in contrast to the maximum value of 4 for the peak-to-pedestal ratio in the case of quantum oscillations without feedback. [37,47]

10. Discussion

The Bayesian formalism discussed in this paper presents (as any formalism of selective quantum evolution [17-36]) a controversy in interpretation. First of all, a natural question is how it is possible that the qubit density matrix evolution can be described simultaneously by the conventional equations (14)-(15) and the Bayesian equations (25)-(26) [and even also by the improved Bayesian equations (64)-(65)]. Which equations are correct? The answer is: all are correct depending on the problem considered.

If only the ensemble evolution is studied (for example, the ensemble of particles is measured, as in typical nuclear magnetic resonance experiments) then the conventional approach is completely sufficient. It is also possible to use the Bayesian equations; however, they should be averaged over all possible measurement results, after which they coincide with the conventional equations. So, the selective approach does not have real advantages for the study of the averaged evolution (besides a significant computational gain in some cases [17-19]). There is still no advantage even for the majority of experiments with individual quantum systems (see examples in Section 2) *if* the averaging is done over a number of repeated experiments, disregarding the results of individual measurements (more exactly, when not more than one number is recorded as a result of each run).

The principal advantage of the selective evolution approach arises for continuous measurement of an individual quantum system when the continuous detector output $I(t)$ is recorded (or at least two numbers are recorded in each run). In this case the selective approach gives the possibility to make

experimental predictions, unaccessible for the conventional approach. The proposals of such experiments with solid-state qubits have been dis- cussed, for example, in Ref. [33] for a one-detector setup and in Ref. [38] for a two-detector setup (the latter experiment seems to be realizable at the present-day level of solid-state technology).

In this case the density matrices calculated by the conventional and Bayesian equations are significantly different. However, they do not contradict each other but rather the Bayesian-calculated density matrix is more accurate than the conventional counterpart. For example, there are no situations when two approaches predict different pure states of the qubit — then it would be possible to prove experimentally than one of the approaches is wrong. In-stead, in a typical situation the conventional equations give a significantly mixed state (so, essentially no predictions are possible) while the Bayesian equations give a pure state (and so some predictions with 100% certainty are possible). A similar relation holds between Bayesian equations (25)?(26) and the improved Bayesian equations (64)-(65): the latter give a more accurate description of qubit evolution and allow us to make more accurate predictions.

The difference between density matrices calculated in different approaches can be easily understood if we treat density matrix not as a kind of "objective reality" but rather as our knowledge about the qubit state (in accordance with orthodox interpretation of quantum mechanics). Then it is obvious that since Bayesian equations take into account additional information [detector output $I(t)$], they provide us with a more accurate description of the qubit state than the conventional equations.

Another controversial issue is the state collapse due to measurement (here it is more appropriate to mention the mathematical formulation by Lüders [11,20] rather than by von Neumann [10]). The conventional equations are derived without any notion of collapse while the derivation of Bayesian equations requires either implicit or explicit (as in the model of Section 6) use of the collapse postulate. Philosophically, the collapse postulate is almost trivial: when the result of the measurement becomes available, we know for sure that the state of the measured system has changed consistently with the measurement result (even though it is generally impossible to predict the result with certainty). In spite of being trivial, this postulate in the author?s

opinion cannot even in principle be derived dynamically by the deterministic Schrödinger equation because of the intrinsic randomness of the measurement result. In other words, the measurement process cannot be described by the Schrödinger equation alone because this equation is designed for closed systems while a quantum object under measurement is always an open system (even including the detector), since the measurement information is output to the outside world. (The incompatibility between quantum mechanics and "macrorealism" has been discussed, e.g., in Ref. [75].)

Following the orthodox (Copenhagen) interpretation, we can regard collapse not as a real physical process but rather as a convenient formal tool to get correct experimental predictions. In the author's opinion this tool is still irreplaceable (if we leave aside the many-worlds interpretations [76,77]) for the complete description of the quantum realm. (Of course, in many cases the collapse postulate is not necessary as, for example, for the description of decoherence due to interaction with the environment — this problem has been solved with great success by the conventional approach.)

Bayesian equations predict several quite counterintuitive results. For example, even for a qubit with an infinite barrier between localized states, $H = 0$, the continuous measurement by an ideal detector leads to a gradual "flow" of the wavefunction between the states (for an initially coherent qubit). The interpretation of this effect is rather difficult if we treat the wavefunction as objective reality; in contrast, there is no problem with the orthodox interpretation. Most importantly, experimental observation of such effects in solid-state qubits is coming into the reach of present-day technology. These experiments would be extremely important not only for better under- standing of the foundations of quantum theory, but could be also useful in the context of quantum computing.

References

[1] C. Bennett, Phys. Today, Oct. 1995, 24 (1995).

[2] Quantum Theory of Measurement, ed. by J. A. Wheeler and W. H. Zurek (Princeton Univ. Press, 1983).

[3] V. B. Braginsky and F. Ya. Khalili, Quantum measurement (Cambridge Univ. Press, 1992).

[4] D. Giulini at al., Decoherence and the Appearance of a Classical World in Quantum Theory (Sprigner-Verlag, Berlin, 1996).

[5] D. Loss and D. P. DiVincenzo, Phys. Rev. A 57, 120 (1998).

[6] B. E. Kane, Nature 393, 133 (1998).

[7] D. V. Averin, Solid State Comm. 105, 659 (1998).

[8] Yu. Makhlin, G. Sch?on, and A. Shnirman, Nature 398, 305 (1999).

[9] J. E. Mooij, T. P. Orlando, L. Levitov, L. Tian, C. H. van der Wal, and S. Lloyd, Science 285, 1036 (1999).

[10] J. von Neumann, Mathematical Foundations of Quantum Mechanics (Princeton Univ. Press, Princeton, 1955).

[11] G. Lüders, Ann. Phys. (Leipzig) 8, 323 (1951).

[12] A. Messiah, Quantum mechanics (Wiley, N.Y., 1961).

[13] A. O. Caldeira and A. J. Leggett, Ann. Phys. (N.Y.) 149, 374 (1983).

[14] U. Weiss, Quantum dissipative systems (World Scientific, Singapore, 1993).

[15] W. H. Zurek, Phys. Today 44 (10), 36 (1991).

[16] E. Joos and H. D. Zeh, Z. Phys. B 59, 223 (1985).

[17] H. J. Carmichael, An open system approach to quantum optics, Lecture notes in physics (Springer, Berlin, 1993).

[18] M. B. Plenio and P. L. Knight, Rev. Mod. Phys. 70, 101 (1998).

[19] M. B. Mensky, Phys. Usp. 41, 923 (1998).

[20] N. Gisin, Phys. Rev. Lett. 52, 1657 (1984).

[21] P. Zoller, M. Marte, and D. F. Walls, Phys. Rev. A 35, 198 (1987).

[22] L. Diosi, J. Phys. A 21, 2885 (1988).

[23] V. P. Belavkin and P. Staszewsky, Phys. Rev. A 45, 1347 (1992).

[24] J. Dalibard, Y. Castin, and K. Molmer, Phys. Rev. Lett. 68, 580 (1992).

[25] N. Gisin and I. C. Percival, J. Phys. A 25, 5677 (1992).

[26] H. M. Wiseman and G. J. Milburn, Phys. Rev. A 47, 1652 (1993).

[27] M. J. Gagen, H. M. Wiseman, and G. J. Milburn, Phys. Rev. A 48, 132 (1993).

[28] G. C. Hegerfeldt, Phys. Rev. A 47, 449 (1993).

[29] R. B. Griffiths, Phys. Rev. Lett. 70, 2201 (1993).

[30] H. M. Wiseman, Phys. Rev. A 49, 2133 (1994).

[31] T. Calarco and R. Onofrio, Phys. Lett A 198, 279 (1995).

[32] C. Presilla, R. Onofrio, and U. Tambini, Ann. Phys. 248, 95 (1996).

[33] A. N. Korotkov, Phys. Rev. B 60, 5737 (1999).

[34] A. C. Doherty and K. Jacobs, Phys. Rev. A 60, 2700 (1999); A. C. Doherty, S. Habib, K. Jacobs, H. Mabuchi, and S. M. Tan, Phys. Rev. A 62, 012105 (2000).

[35] A. N. Korotkov, Physica B 280, 412 (2000).

[36] H.-S. Goan, G. J. Milburn, H. M. Wiseman, and H. B. Sun, e-print cond-mat/0006333.

[37] A. N. Korotkov, e-print cond-mat/0003225.

[38] A. N. Korotkov, e-print cond-mat/0008003.

[39] S. A. Gurvitz, Phys. Rev. B 56, 15215 (1997).

[40] Actually, for $S_1 \neq S_2$ the signal-to-noise ratio corresponding to τ_m defined by Eq. (5) is not exactly unity; however, it has the desired asymptotic behavior $(t/\tau_m)^{1/2}$ at $t/\tau_m \gtrsim |\ln(S_1/S_2)|$. Notice that a reliable measurement result can be obtained only after several times τ_m ($2\tau_m$ gives 98% reliability, $3\tau_m$ gives 99.9%, etc.).

[41] E. Buks, R. Schuster, M. Heiblum, D. Mahalu, and V. Umansky, Nature 391, 871 (1998).

[42] D. Sprinzak, E. Buks, M. Heiblum, and H. Shtrikman, Phys. Rev. Lett. 84, 5820 (2000).

[43] I. L. Aleiner, N. S. Wingreen, and Y. Meir, Phys. Rev. Lett. 79, 3740 (1997).

[44] Y. Levinson, Europhys. Lett. 39, 299 (1997).

[45] L. Stodolsky, Phys. Lett. B 459, 193 (1999).

[46] G. Hackenbroich, B. Rosenov, H. A. Weidenmüller, Phys. Rev. Lett. 81, 5896 (1998).

[47] A. N. Korotkov and D. V. Averin, e-print cond-mat/0002203.

[48] D. V. Averin, e-print cond-mat/0004364.

[49] G. B. Lesovik, JETP Lett. 49, 591 (1989).

[50] A. Shnirman and G. Schön, Phys. Rev. B 57, 15400 (1998).

[51] Y. Nakamura, Yu. A Pashkin, and J. S. Tsai, Nature 398, 786 (1999).

[52] D. V. Averin and K. K. Likharev, in Mesoscopic Phenomena in Solids, edited by B. L. Altshuler, P. A. Lee, and R. A. Webb (Elsevier, Amsterdam, 1991), p. 173.

[53] By coincidence, the word "orthodox" is used for both Copenhagen interpretation of quantum mechanics and for the semiclassical theory of correlated single-electron tunneling.

[54] A. N. Korotkov, D. V. Averin, K. K. Likharev, and S. A. Vasenko, in Single-Electron Tunneling and Mesoscopic Devices, edited by H. Koch and H. Lübbig (Springer, Berlin, 1992), p. 45.

[55] A. N. Korotkov, Phys. Rev. B 49, 10381 (1994).

[56] J. R. Friedman, V. Patel, W. Chen, S. K. Tolpygo, and J. E. Lukens, Nature 406, 43 (2000); S. Han, J. Lapointe, and J. E. Lukens, Phys. Rev. Lett. 66, 810 (1991).

[57] K. K. Likharev, Dynamics of Josephson junctions and circuits (Gordon and Breach, New York, 1986).

[58] M. Scully and W. E. Lamb, Phys. Rev. Lett 16, 853 (1966).

[59] R. A. Harris and L. Stodolsky, J. Chem. Phys. 74, 2145 (1981).

[60] Yu. Makhlin, G. Schön, and A. Shnirman, e-print cond-mat/0001423.

[61] V. V. Danilov, K. K. Likharev, and A. B. Zorin, IEEE Trans. Magn. MAG-19, 572 (1983).

[62] Yu. Makhlin, G. Schön, and A. Shnirman, e-print cond-mat/9811029.

[63] S. A. Gurvitz, e-print quant-ph/9808058.

[64] T. Bayes, Phil. Trans. Royal Soc. 53, 370 (1763)

[65] E. Borel, Elements of the theory of probability (Prentice-Hall, N.J., 1965).

[66] Notice that the noise spectral density S_0 is treated in the Bayesian formalism as frequency-independent. This implies that we do not consider frequencies higher than the typical frequency ω_0 above which S_0 becomes frequency-dependent.

[67] B. Oksendal, Stochastic differential equations (Springer, Berlin, 1998).

[68] In a more general case of an arbitrary detector with the possibility to observe each passing electron, Eqs. (48)-(49) remain valid, so using the inequality $|\rho_{12}|^2 \leq \rho_{11}\rho_{22}$ and ensemble averaging we obtain the lower bound $\Gamma_d \geq (\sqrt{I_1} - \sqrt{I_2})^2/2e$. If the Schottky formula is still applicable, $S_i = 2eI_i$, this makes the general inequality $2\Gamma_d\tau_m \geq 1$ valid even outside the weakly responding regime.

[69] At the first glance the condition $\Delta t_k \gg e/I_{1,2}$ seems to be sufficient for the equivalence between the two results. However, if I_i and I_2 are significantly different, then the averaging of $\rho_{12}(t)$ gives different results in the two models (see remark 28 in Ref. [33]). This is because the tails of Poissonian and Gaussian distributions are different even when the central parts coincide well.

[70] In a model with an effectively finite number of detector degrees of freedom the collapse by the pointer would disturb the interaction between qubit and detector; in particular, sufficiently frequent collapse could lead to Quantum Zeno freezing of the detector state. For example, for a finite-transparency quantum point contact the "attempt frequency" $eV/\hbar$ is always comparable to the typical frequency I/e of electron passage. As a consequence, a readout often and strong enough to observe individual electrons, $\Delta t_k \lesssim e/I$, would necessarily disturb the measurement process.

[71] The small shift of the detector operating point for two localized qubit states can affect the energy ε, which therefore should be defined self-consistently.

[72] A. B. Zorin, Phys. Rev. Lett. 76, 4408 (1996).

[73] D. V. Averin, e-print quant-ph/0008114.

[74] A. Maassen van den Brink, e-print quant-ph/0009163.

[75] A. J. Leggett and A. Garg, Phys. Rev. Lett. 54, 857 (1985); 54, 2724 (1985); 59, 1621 (1987); 63, 2159 (1989).

[76] H. Everett, Rev. Mod. Phys. 29, 454 (1957).

[77] B. S. De Witt, Phys. Today 23 (9), 30 (1970).